Motorcycle State Estimation and Tire Cornering Stiffness Identification Applied to Road Safety: Using Observer Based Identifiers

Majda FOUKA, Lamri NEHAOUA and Hichem ARIOUI

***Abstract*—This paper deals with observer-based identification framework to estimate both lateral dynamic states and tires' cornering parameters in the perspective of designing advanced rider assistance systems for powered two-wheeled vehicle. An adaptive observer is proposed to reconstruct the state variables regardless the forward velocity variations and to estimate the real unknown tires' parameters. The stability and convergence analysis of the proposed observer is based on the Lyapunov theory, the persistency of excitation and the general Lipschitz condition. To enable this observer design, the linear parameter varying observer is transformed into Takagi-Sugeno exact form observer where the sufficient conditions are given in terms of linear matrix inequalities. Finally, an evaluation framework is proposed to provide a critical overview about the method effectiveness. The proposed adaptive law is compared to a direct estimation and a dynamic inversion estimation methods. Co-simulation scenarios are performed by using both BikeSim© motorcycle simulator and real data-log obtained from an instrumented electrical scooter.**

***Index Terms*—Adaptive LPV Observer, Motorcycle safety, Lateral dynamics, State estimation, Tire Parameters identification.**

I. Introduction

The technological achievement of the powered two-wheeled vehicle (PTWv) and its expansion not just conveyed a funny transportation system to their users through a noteworthy decrease time, but also has introduced a genuine and complex safety challenges. Unlike car vehicles, the integration of the various safety into one architecture can lead to an unexpected behavior in hazard riding situations. The supply of road safety for PTWv riders remains useless as long as some driving rules are not always adapted to riding psycho-physical capacity like the visual fields, distance assessment, dynamics evaluation and loss of attention. Therewith, the development of advanced driver assistance systems (ADAS) to improve rider safety should integrate riding experience and vehicle controllability in different driving situations.

Developing ADAS for PTWv remains a high theoretical and technical challenge. The self-unstable characteristic of PTWv gives rise to various difficulties in design, control, estimation, rider behavior analysis and effectiveness assessment. Indeed, ADAS systems depend basically on motorcycle motion states as steering behavior, roll angle and tire/road interaction. The evolution of these states depends strongly on the riders' actions and vehicle's parameters such that rider's torque applied on the motorcycle handlebar, tire cornering stiffness, PTWv mass and inertia moment. Hence, build up an ADAS requires a precise knowledge, at every instant, of the vehicle's dynamics throughout physical or virtual sensors. This topic is one of our research interest which intends to develop ADAS systems starting from a minimum set of self vehicle integrated sensors to acquire measured states. For the remaining unmeasured, model-based state estimators are used to achieve a reliable estimation of both the vehicle's unmeasured dynamics and the most important unknown parameters. One of the important unknown parameters are tires' stiffness. In fact, the main goal of ADAS is to handle the vehicle before reaching the limits of its stability region which is mainly depends on the tire/road generated longitudinal and lateral forces with respect to the road available friction. The PTWv's rider should be aware at each instant about the available road friction and the optimal turn speed to avoid an over-steer or an under-steer behavior. This enables to foresee the ideal roll angle required to generate the lateral forces.

An extensive research effort has been done to examine the effectiveness of various estimation and identification methods in improving handling and stability of PTWv [1], [2], [3], [4], [5]. In almost references, the estimation of the PTWv dynamics is done by considering restrictive assumptions with respect to riding practice, parameters variation interval, and also by considering a known tire friction or under a constant speed assumption [6], [7]. These assumptions simplify the estimation problem but lead to an inaccurate estimation with respect to the real dynamics. In fact, motorcycle characteristics and road conditions may change for different riding situations. Therefore, it is interesting to estimate a set of optimal system's parameters from the available input-output data and a prior knowledge about the system's behavior. In [8], a survey on vehicle dynamic states estimation is proposed where the estimation methods advantages and shortcomings are highlighted. In the framework of the vehicle control, a disturbance observer is proposed in order to achieve both the desired side-slip angle and the yaw rate. Also, in [9], an interval fault estimation approach by using zonotopic technique is proposed. A discrete-time linear parameter-varying systems is considered in the presence of bounded parametric uncertainties, measured perturbation, and system disturbance. However, the direct transposition of almost approaches developed for four-wheeled vehicles remains a great challenge.

To the authors' best knowledge, a very few works deals with

This work has been supported by ANR project : VIROLO++ and *Informatics, Integrative Bio-Informatics and Complex Systems Laboratory* (IBISC), *Evry Val d'Essonne (UEVE)- Paris-Saclay University*. Majda Fouka, Lamri Nehaoua and Hichem Arioui are with the IBISC LAB, UEVE-Paris Saclay University, 43 Rue du Pelvoux, 91080 Courcouronnes, France. Email: {majda.fouka}@univ-evry.fr.

the PTWv parameters identification, which use regression-based estimation methods to recover the road available friction or the vehicle's parameters [10], [11]. These methods are designed under consideration for a specific systems form and their direct transposition to the more general problem case is not straightforward for many reason. First, the identification problem is formulated assuming that all the system states are measured, which is really untruthfully. Second, the parameter identification problem is closely related to persistency of excitation that can reach an optimal solution [12]. Moreover, for identification process, suitable rich input signals should be considered, while in practice, these signals can not be freely applied to excite the PTWv due to the system constraints, and lead to a set of incompatible parameters. Alternative approaches suggest the use of observer-based identification. In this scope, adaptive observers present a convenient approach to deal with both dynamic states and parameters estimation [13]. In [14], an adaptive robust observer is designed for a class of parametric semi-strict feedback nonlinear systems. And in [15], a nonlinear high gain observer design based on the full-order model of the induction motor is proposed. Such an effort appears nontrivial due to the fact that the full-model at best admits locally a non-triangular observable form. Also, in [16], trajectory tracking has been proposed based on an output-feedback iterative learning controller, together with a state observer and a fully-saturated learning mechanism, through Lyapunov-like synthesis. The focus was on the convergence problem, to deal with time-varying parametric uncertainties.

In the present paper, an estimation framework is proposed for the PTWv dynamic states estimation and tires' stiffness identification by considering the self integrated vehicle's sensor. The proposed approach can be summarized in four steps. First, a nonlinear PTWv dynamics model is described including lateral, yaw, roll and steering motions where the forward speed is considered to be a varying parameter. Next, the dynamics model is written in an LPV form where the state matrix includes only the varying measured parameters and, all unknown parameters are collected in one term which can be written in an affine form for identification purpose. After, an LPV-adaptive observer is proposed and then transformed into Takagi-Sugeno exact form for stability and convergence analysis. Finally, sufficient conditions are given in terms of linear matrix inequalities (LMIs) to enable design. In the best case, this technique allows to make the estimation error asymptotically converge to zero. The design of such observers supposes the availability of the measures and their prior processing. One must keep in mind that this contribution is a more realistic validation toward the experimental testing. The long term objective is to use these estimated informations to design risk function which can be integrated in a warning ADAS system.

This paper is organized in six sections. section II presents the PTWv dynamics. The LPV-adaptive observer design methodology is described in section III with stability analysis. Co-simulation and experimental validation are discussed in section V. Finally, section VII concludes the paper.

II. PTWv DYNAMICS

A. Model description

In this work, the well-known Sharp model is used to describe the PTWv lateral dynamics [17]. The PTWv is represented as a set of two bodies linked by the steering mechanism allowing the simulation of 4 DoF (Degrees of Freedom) as shown in Fig. 1. The main body is subject to lateral motion according to the generated tire forces whereas the front body is subject to steering motion as derived by the applied rider's steering torque on the vehicle's handlebar.

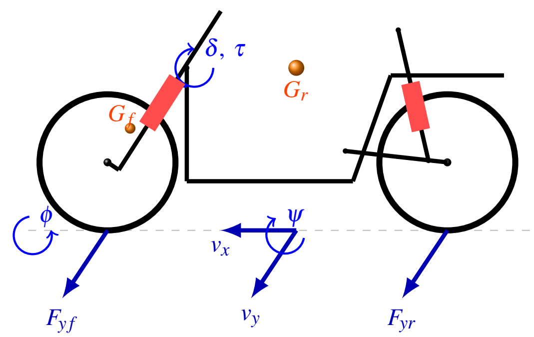

Fig. 1: Geometrical representation of the motorcycle

The lateral, yaw, roll and steering dynamics are respectively described by the following equations :

$$\begin{aligned}
e_{33}\dot{v}_y + e_{34}\ddot{\psi} + e_{35}\ddot{\phi} + e_{36}\ddot{\delta} &= a_{34}\dot{\psi} + F_{yf} + F_{yr} \\
e_{34}\dot{v}_y + e_{44}\ddot{\psi} + e_{45}\ddot{\phi} + e_{46}\ddot{\delta} &= a_{44}\dot{\psi} + a_{45}\dot{\phi} + a_{46}\dot{\delta} \\
&\quad + a_{47}F_{yf} + a_{48}F_{yr} \\
e_{35}\dot{v}_y + e_{45}\ddot{\psi} + e_{55}\ddot{\phi} + e_{56}\ddot{\delta} &= a_{54}\dot{\psi} + a_{56}\dot{\delta} + a_{51}\phi + a_{52}\delta \\
e_{36}\dot{v}_y + e_{46}\ddot{\psi} + e_{56}\ddot{\phi} + e_{66}\ddot{\delta} &= a_{64}\dot{\psi} + a_{65}\dot{\phi} + a_{66}\dot{\delta} + a_{61}\phi \\
&\quad + a_{62}\delta + a_{67}F_{yf} + \tau
\end{aligned} \tag{1}$$

Equations (1) can be written under the following state space:

$$E\dot{x} = \bar{A}(v_x(t))x(t) + \bar{B}u(t) \tag{2}$$

where $x(t) \in \mathbb{R}^{n_x}$ is the state vector including the PTWv dynamics such that $x = [\phi, \delta, v_y, \dot{\psi}, \dot{\phi}, \dot{\delta}, F_{y_f}, F_{y_r}]^T$. The input vector is denoted by $u(t) \in \mathbb{R}$ where $u(t) = \tau(t)$ refers to the rider's torque. The vehicle's forward speed $v_x(t)$ is considered as a measured time-varying parameter. The matrix $E = [e_{ij}] \in \mathbb{R}^{n_x \times n_x}$ is constant and invertible, $\bar{A} = [\bar{a}_{ij}] \in \mathbb{R}^{n_x \times n_x}$ is a time-varying matrix depending on $\zeta(t)$ and the unknown tire parameters. $\bar{B} \in \mathbb{R}^{n_x}$ is a constant vector. All matrices and parameters are defined in tables VI, V and IV.

In addition to the motion dynamics, we introduce the tire relaxation to characterize the transient behavior by means of a first order system as following:

$$\frac{\sigma}{v_x}\dot{F}_{y_k} = -F_{y_k} + F_{y_k}^{SS} \qquad k = f, r \tag{3}$$

where, $F_{y_k}^{SS}$ are the steady state lateral tires' forces generated according to the tire's side-slip angle α_k and the camber angle

γ_k. σ_k is the tire's relaxation. In steady state, these forces are given by the following linear equation:

$$F_{y_k}^{SS} = -C_{\alpha_k}\alpha_k + C_{\gamma_k}\gamma_k \tag{4}$$

where, side-slip angle α_k and the camber angle γ_k, for the front and rear tire, are given by [17]:

$$\begin{aligned} \alpha_f &= \frac{v_y + l_f\dot{\psi}}{v_x} - \delta\cos\varepsilon \qquad & \alpha_r &= \frac{v_y - l_r\dot{\psi}}{v_x} \\ \gamma_f &= \phi + \delta\sin\varepsilon & \gamma_r &= \phi \end{aligned} \tag{5}$$

The use of a linear tire representation is justified as is discussed in the introduction section. ADAS are dedicated to perform safety tasks before the vehicle reaches the limits of its stability region. Beyond the stability region, almost ADAS fails to recover the vehicle handling.

B. Parameter-dependent model

Let consider $\zeta(t) = v_x(t)$ a varying measured parameter and $\Theta \in \mathbb{R}^{n_\Theta}$ is the unknown parameters vector. The PTWv model of equation (2) can be reformulated in the following LPV form:

$$\begin{cases} \dot{x} = A_\zeta x + Bu + \Lambda(x,\zeta,\Theta) \\ y = Cx \end{cases} \tag{6}$$

where $y \in \mathbb{R}^{n_y}$ is the output measured vector and $\Lambda(x,\zeta,\Theta) \in \mathbb{R}^{n_x}$ represents the parameters of the PTWv dynamics.

In fact, we introduce $C_{s_k,0}$, the nominal values of the tires' stiffness where $s = \alpha,\gamma$. Equation (3) can be written as:

$$\begin{aligned} \frac{\sigma}{v_x}\dot{F}_{yk} = -F_{yk} + C_{\alpha_k,0}\alpha_k + C_{\gamma_k,0}\gamma_k + \\ (C_{\alpha_k} - C_{\alpha_k,0})\alpha_k + (C_{\gamma_k} - C_{\gamma_k,0})\gamma_k \end{aligned} \tag{7}$$

By replacing α_k and γ_k by their respective expressions from equation (5) in the previous equation, we get:

$$\begin{aligned} \begin{bmatrix} \dot{F}_{yf} \\ \dot{F}_{yr} \end{bmatrix} &= \begin{bmatrix} a_{71,0} & a_{72,0} & a_{73,0} & a_{74,0} & 0 & a_{76,0} & a_{77,0} & 0 \\ a_{81,0} & 0 & a_{83,0} & a_{84,0} & 0 & 0 & 0 & a_{88,0} \end{bmatrix} x + \\ & \underbrace{\begin{bmatrix} -\frac{v_x\alpha_f}{\sigma_f} & \frac{v_x\gamma_f}{\sigma_f} & 0 & 0 \\ 0 & 0 & -\frac{v_x\alpha_r}{\sigma_r} & \frac{v_x\gamma_r}{\sigma_r} \end{bmatrix}}_{\chi(x,\zeta)} \underbrace{\begin{bmatrix} C_{\alpha_f} - C_{\alpha_f,0} \\ C_{\gamma_f} - C_{\gamma_f,0} \\ C_{\alpha_r} - C_{\alpha_r,0} \\ C_{\gamma_r} - C_{\gamma_r,0} \end{bmatrix}}_{\Theta} \end{aligned} \tag{8}$$

where $a_{ij,0}$ are the parameters a_{ij} of matrix $\bar{A}(\zeta)$ evaluated for the nominal values of the tires' stiffness $C_{s_k,0}$. After some algebraic manipulations, equation (6) is recovered in which:

$$\begin{aligned} A_\zeta &= E^{-1}\bar{A}(\zeta) \\ B &= E^{-1}\bar{B} \\ \Lambda(x,\zeta,\Theta) &= D\chi(x,\zeta)\Theta \\ D &= E^{-1}\begin{bmatrix} 0_{6,2} \\ I_2 \end{bmatrix} \end{aligned} \tag{9}$$

where $0_{6,2} \in \mathbb{R}^{6,2}$ a zero matrix and $I_2 \in \mathbb{R}^{2,2}$ is an identity matrix. An inertial measurement unit (IMU) is embedded on the PTWv and mounted under the vehicle's seat at approximately the vehicle's center of mass. The available measurements are three accelerations and three angular velocities expressed in the IMU body reference frame. These measurements are used to derive the roll angle rate $\dot{\phi}$, yaw angle rate $\dot{\psi}$ and the lateral acceleration a_y expressed in the PTWv modeling reference frame. In addition to the IMU measurement, an optical encoder is fixed on the steering body providing the steering angle δ and its time-derivative $\dot{\delta}$. The minimum set of sensor measurements are the following:

$$y = \begin{bmatrix} \delta & \dot{\psi} & \dot{\phi} & \dot{\delta} & a_y \end{bmatrix}^T \tag{10}$$

C. Problem statement

From PTWv dynamics equation, it is straightforward to find an approximate estimation of the tires' cornering stiffness using a direct method or a dynamics inversion approach. With the direct method [18], the PTWv can be reduced to an equivalent one-body dynamics expressed by:

$$\begin{cases} Ma_y = F_{yf} + F_{yr} \\ I_z\ddot{\psi} = l_f F_{yf} - l_r F_{yr} \end{cases} \tag{11}$$

where M and I_z are the PTWv's equivalent body mass and z-inertia. By combining equations (4), (3) and (11), we get:

$$\begin{bmatrix} -\alpha_f & \gamma_f & -\alpha_r & \gamma_r \\ -l_f\alpha_f & l_f\gamma_f & l_r\alpha_r & -l_r\gamma_r \\ -\alpha_f & \gamma_f & 0 & 0 \\ 0 & 0 & -\alpha_r & \gamma_r \end{bmatrix} \begin{bmatrix} C_{\alpha_f} \\ C_{\gamma_f} \\ C_{\alpha_r} \\ C_{\gamma_r} \end{bmatrix} = \begin{bmatrix} Ma_y \\ I_z\ddot{\psi} \\ \frac{\sigma_f}{v_x}\dot{F}_{yf} + F_{yf} \\ \frac{\sigma_r}{v_x}\dot{F}_{yr} + F_{yr} \end{bmatrix} \tag{12}$$

In the other hand, the dynamics inversion gives more insight in parameters estimation by avoiding state differentiation as in equation (12). This method is based on classical unknown input observers and output differentiation as reported in [19], [20]. From equations (6) and (9), we get:

$$\dot{\hat{y}} = CA_\zeta\hat{x} + CBu + CD\chi(\hat{x},\zeta)\hat{\Theta} \tag{13}$$

By an algebraic inversion of the previous equation leads to a state estimation without the need of parameters identification and the unknown parameters vector Θ can be reconstructed from the estimation of the state vector and output derivatives. However, the feasibility of this inversion is conditioned by a convenient selection of the excitation signal to fulfill rank condition rank(CD) =rank(D).

The problem of state estimation and unknown parameters identification of the motorcycle dynamics is addressed. The front and rear tires' cornering stiffness identification are the focus of our interest since they play a key role to guarantee the motorcycle stability in turns maneuvers. Moreover, it is known among all vehicle dynamics literature that tires' cornering stiffness are combined with the available road friction μ, then, solving the estimation problem for the unknown parameters vector Θ is equivalent to finding the combined vector $\Theta = \mu\Theta_0$, where Θ_0 is the tires' nominal stiffness. Without loss of generality, in this paper the tires' cornering stiffness are considered with their associated road friction are embedded in one variable. For some very special cases such a puddle and dead leaf causing an abrupt variation of road friction, the problem of friction estimation can be more efficiently solved by using other techniques like that vision-based classification [21], [22].

III. Observer design

In this section, the design of the LPV-adaptive observer is described based on the PTWv model of equation (6). Next, asymptotic convergence is proved by using Lyapunov theory associated with the Lipschitz property, giving rise to an optimization problem expressed by a set of LMI to be solved.

A. Observability Analysis

The PTWv model referenced by equation (6) with its associated output measurements vector does not satisfy the observability/detectability condition. One solution is to use the flatness properties [23] to define additional virtual measurements [24]. From equations (2), we consider the lateral and yaw dynamics given by:

$$\begin{bmatrix} E_{3,:} \\ E_{4,:} \end{bmatrix} \dot{x} = \begin{bmatrix} \bar{A}_{3,:} \\ \bar{A}_{4,:} \end{bmatrix} x \tag{14}$$

where the notation $E_{i,:}$ denotes the i^{th} line of matrix E. After some algebraic manipulations, the output measurements vector y, equation (6), can be augmented with an auxiliary virtual sensor output, y_a, expressed by:

$$y_a = (M_f k - M l_f) F_{yf} + (M_f k + M l_r) F_{yr} \tag{15}$$

B. LPV-adaptive observer

Assumption 1. Assume that $\zeta \in \Delta$ be a set of vectors defined on an hyper-rectangles Δ given by:

$$\Delta = \left\{ \zeta \in \mathbb{R}^{n_\zeta} \middle| \ \zeta_{i_{min}} \leq \zeta_i \leq \zeta_{i_{max}} \ \right\} \tag{16}$$

Assumption 2.

- The system's input $u(t)$ is known and sufficiently persistent, i.e, it exists constants c_1, c_2 and c_3 such that for all t the following inequality holds [25] :
$$c_1 I \leq \int_{t_0}^{t_0+c_3} D\chi(\hat{x}, v_x)\chi^T(\hat{x}, v_x)D^T dt \leq c_2 I$$
- The state vector $x(t)$ and the input vector $u(t)$ are bounded. This assumption will fit the general practical case, *e.g.* a stable motion of a PTWv.

Theorem 1. Given the PTWv dynamics of equation (2) satisfying assumptions (1-2), the following LPV-adaptive observer:

$$\begin{cases} \dot{\hat{x}} = A_\zeta \hat{x} + Bu + \Lambda(\hat{x}, \zeta, \hat{\Theta}) + L_\zeta(y - \hat{y}) \\ \hat{y} = C\hat{x} \end{cases} \tag{17}$$

with the adaptation law:

$$\dot{\hat{\Theta}} = \Gamma \chi^T(\hat{x}, \zeta) T C \tilde{x} \quad \text{and} \quad \Gamma = \Gamma^T > 0 \tag{18}$$

ensures an asymptotic convergence error for the simultaneous state and parameters vector estimation, toward zero if there exist a symmetric positive definite matrix P and matrices K_ζ and R satisfying the following inequalities :

$$PA_\zeta + A_\zeta^T P - K_\zeta C - C^T K_\zeta^T + PQ^{-1}P^T + R < 0 \tag{19}$$

$$D^T P = TC \tag{20}$$

where $\tilde{x}$ is the state estimation error vector and L_ζ is the observer gain matrix .

Proof 1. Lets consider the following LPV-adaptive observer :

$$\begin{cases} \dot{\hat{x}} = A_\zeta \hat{x} + Bu + \Lambda(\hat{x}, \zeta, \hat{\Theta}) + L_\zeta(y - \hat{y}) \\ \hat{y} = C\hat{x} \end{cases} \tag{21}$$

where $\hat{x}$, $\hat{y}$ and $\hat{\Theta}$ are respectively the estimated state, output and parameters vector. L_ζ is the observer gain matrix such that $\Phi_\zeta = A_\zeta - L_\zeta C$ is Hurwitz. Lets $\tilde{x} = x - \hat{x}$ and $\tilde{\Theta} = \Theta - \hat{\Theta}$ be respectively the state and the parameters estimation error vector. The error dynamics can be computed as following:

$$\dot{\tilde{x}} = \Phi_\zeta \tilde{x} + \tilde{\Lambda} + D\chi(\hat{x}, \zeta)\tilde{\Theta} \tag{22}$$

in which $\tilde{\Lambda} = \Lambda(x, \zeta, \Theta) - \hat{\Lambda}(\hat{x}, \zeta, \Theta)$.

The stability analysis can be performed by considering the following quadratic Lyapunov function :

$$V(\tilde{x}) = \tilde{x}^T P \tilde{x} + \tilde{\Theta}^T \Gamma^{-1} \tilde{\Theta} \tag{23}$$

where P and Γ are symmetric positive definite matrices.

By taking the time derivative of the Lyapunov function (23), and replacing the state estimation error dynamics by its equation (22), we obtain:

$$\begin{aligned} \dot{V} = & \tilde{x}^T \Psi_\zeta \tilde{x} + \tilde{\Lambda}^T P^T \tilde{x} + \tilde{x}^T P \tilde{\Lambda} + \tilde{\Theta}^T \Gamma^{-1} \dot{\tilde{\Theta}} + \dot{\tilde{\Theta}}^T \Gamma^{-1} \tilde{\Theta} \\ & + \tilde{\Theta}^T \chi^T(\hat{x}, \zeta) D^T P \tilde{x} + \tilde{x}^T P D \chi(\hat{x}, \zeta) \tilde{\Theta} \end{aligned} \tag{24}$$

where $\Psi_\zeta = \Phi_\zeta^T P^T + P\Phi_\zeta$.

Lets consider the following lemmas:

Lemma 1. The function $\Lambda(x, \zeta, \Theta)$ is said to be Lipschitz [26] with respect to x, if for all x, the function $\Lambda(x, \zeta, \Theta)$ can be rewritten under the following generalized Lipschitz condition:

$$\Lambda^T Q \Lambda \leq x^T R x \tag{25}$$

where Q and R are respectively symmetric positive and semi-positive definite matrices. Thus, any system in the form of equation (6), can be reformulated in a generalized Lipschitz condition, as long as $\Lambda(x, \zeta, \Theta)$ is continuously differentiable with respect to x.

Lemma 2. For every matrix G, symmetric positive definite, the following property holds [27]:

$$X^T Y + Y^T X \leq X^T G X + Y^T G^{-1} Y$$

By using the Lipschitz condition in lemma (1) and the property in lemma (2), we get the following inequality :

$$\tilde{\Lambda}^T P^T \tilde{x} + \tilde{x}^T P \tilde{\Lambda} \leq \tilde{x}^T P Q^{-1} P^T \tilde{x} + \tilde{\Lambda}^T Q \tilde{\Lambda} \tag{26}$$

Now, we can prove exponential stability convergence:

$$\begin{aligned} \dot{V}(t) \leq & \tilde{x}^T \left(\Psi_\zeta + PQ^{-1}P^T + R\right) \tilde{x} + \tilde{\Theta}^T \chi^T(\hat{x}, \zeta) D^T P \tilde{x} + \\ & \tilde{x}^T P D \chi(\hat{x}, \zeta) \tilde{\Theta} + \tilde{\Theta}^T \Gamma^{-1} \dot{\tilde{\Theta}} + \dot{\tilde{\Theta}}^T \Gamma^{-1} \tilde{\Theta} \end{aligned} \tag{27}$$

Following assumption (2), in the case of a stable PTWv dynamics with a bounded states, the estimated term $\chi(\hat{x}, \zeta)$ will be bounded by an upper singular values, e.g., $\|\chi(\hat{x}, \zeta)\|_2 < \sigma_{\max}$. Consequently:

$$\dot{V}(t) \leq \tilde{x}^T \left(\Psi + PQ^{-1}P^T + R\right) \tilde{x} + 2\tilde{\Theta}^T \Gamma^{-1} \dot{\tilde{\Theta}} + 2\sigma_{\max} \tilde{\Theta}^T D^T P \tilde{x} \tag{28}$$

At this level, we can derive the observer's adaptive law from equation (28) as following:

$$\tilde{\Theta}^T \Gamma^{-1} \dot{\tilde{\Theta}} + \sigma_{\max} \tilde{\Theta}^T D^T P \tilde{x} < 0 \tag{29}$$

According to the tire's relaxation formula (3), the unknown parameters rate is practically slow, *e.g.* $\dot{\Theta} = 0$ and hence, $\dot{\tilde{\Theta}} = -\dot{\hat{\Theta}}$. Furthermore, it is possible to find a matrix T, such that $D^T P = TC$ [28]. The adaptive law can be stated as:

$$\dot{\hat{\Theta}} = \Gamma \chi^T(\hat{x}, \zeta) TC\tilde{x} \quad \text{and} \quad \Gamma = \Gamma^T > 0 \tag{30}$$

With this law, the time derivative $\dot{V}(t)$ becomes :

$$\dot{V}(t) \leq \tilde{x}^T (A_\zeta^T P^T + PA_\zeta - C^T K_\zeta^T - K_\zeta C + PQ^{-1} P^T + R)\tilde{x} \tag{31}$$

where $K_\zeta = PL_\zeta$.

C. Polytopic form

Theorem (1) in section (III) introduces a theoretical framework for the states and parameters estimation. The resulting optimization problem, given by the inequality of equation (19), is parameter dependent, thus, we must revisit our observer.

Theorem 2. The following LPV-adaptive observer :

$$\begin{cases} \dot{\hat{x}} = A_\zeta \hat{x} + Bu + \Lambda\left(\hat{x}, \zeta, \hat{\Theta}\right) + L_\zeta (y - C\hat{x}) \\ \dot{\hat{\Theta}} = \sigma_{\max} \tilde{\Theta}^T D^T P \tilde{x} \end{cases} \tag{32}$$

ensures an asymptotic convergence of the state estimation error for system class of equation 2, if and only if there exist a matrix P symmetric positive definite, a matrix K_ζ, and a matrix R satisfying the Liptchiz condition. Thus, if the condition $rank(CD) = rank(D)$ is fulfilled, a matrix Γ symmetric positive definite can be found such that the following LMIs hold:

$$\min_{i=1,\cdots,r} \varsigma \quad \text{s.t.}$$

$$\begin{bmatrix} \varsigma I & D^T P - TC \\ (D^T P - TC)^T & \varsigma I \end{bmatrix} \succ 0 \tag{33}$$

$$\begin{bmatrix} A_i^T P + PA_i - C^T K_i^T - K_i C + R & P \\ P & -Q \end{bmatrix} \prec 0 \tag{34}$$

Proof 2. The PTWv model in equation (2) is dependent on the measured vehicle's speed, e.g., $\zeta = v_x$. According to assumption (1), and knowing that ζ satisfies the following convex property:

$$\sum_{i=1}^{r} \eta_i(\zeta) = 1, \quad 0 \leq \eta_i(\zeta) \leq 1 \tag{35}$$

where η_i are weighting functions. By using the so-called Takagi-Sugeno (TS) structure [29], the PTWv model in equation (2) can be reformulated as a set of interconnected linear time invariant models. Since the model depends on non-linearity $\zeta \in \Delta$, supposed to be accessible at real-time, the resulting LPV model (6) in TS structure is described by 2 sub-models as:

$$\begin{cases} \dot{x} = \sum_{i=1}^{r} \eta_i(\zeta) A_i x + Bu + \Lambda(x, \zeta, \Theta) \\ y = Cx \end{cases} \tag{36}$$

where $r = 2^{n_\zeta}$ is the number of the sub-models corresponding to n_ζ non-linearities ($n_\zeta = 1$ in our case). Then, A_ζ in equation (2) becomes $\sum_{i=1}^{r} \eta_i(\zeta) A_i$ and A_i are constant matrices.

From theorem (1) and using the convex sum property of the weighting functions, sufficient conditions ensuring $\dot{V}(t) < 0$ are established by the following LMIs:

$$A_i^T P + PA_i - C^T K_i^T - K_i C + PQ^{-1} P^T + R < 0 \tag{37}$$

By applying Schur lemma, inequality (19) can be transformed to the second LMI of equation (33). The observer gain matrix L in theorem (2) is also defined by:

$$\begin{cases} K_\zeta = \sum_{i=1}^{r} \eta_i(\zeta) K_i, \\ L_\zeta = \sum_{i=1}^{r} \eta_i(\zeta) L_i, \\ L_i = P^{-1} K_i \end{cases} \tag{38}$$

Finally, the equality constraint $D^T P = TC$ can be formulated by the optimization problem described by equation (33).

IV. Simulation results

In this section, the effectiveness of the proposed estimation framework is investigated by co-simulation with Bikesim© software [30]. The PTWv model *Scooter Big Baseline* is chosen from the software dataset, in which, the nominal values $C_{j_i,0}$ of the lateral slip and camber stiffness are available. The test scenario is carried out by considering a handling maneuver depicted in Fig. 2c and involving a medium hard rider torque represented in Fig. 2a. The forward speed is a measured varying parameter ranging from 40 km/h to 120 km/h as shown in Fig. 2a. For this first setup, the road friction coefficient is fixed to a constant value $\mu = 0.9$. The observer gains L_i are computed using theorem 2 and the motorcycle parameters listed in Table VI. The test scenario is in accordance with a real regular riding condition. It also allows to highlight the observer performance by covering a broad spectrum of the PTWv dynamics within and beyond its linearization domain. Further, we test the adaptive law with a constant gain matrix Γ and with zero initial condition.

Fig. 3a shows the state estimation performance with respect to their measured values from Bikesim and also demonstrates a finite-time asymptotic estimation. Furthermore, since the lateral velocity v_y, the roll angle ϕ and tire forces F_{yf}, F_{yr} are unmeasurable, their estimations are used to reconstruct the lateral acceleration a_y at the center of mass of the rear body G_r by using the two equations in (39). Fig. 3c represents the estimated lateral acceleration and the corresponding one given by Bikesim. It is obvious that these results show finite-time asymptotic estimation where exact estimation can't be

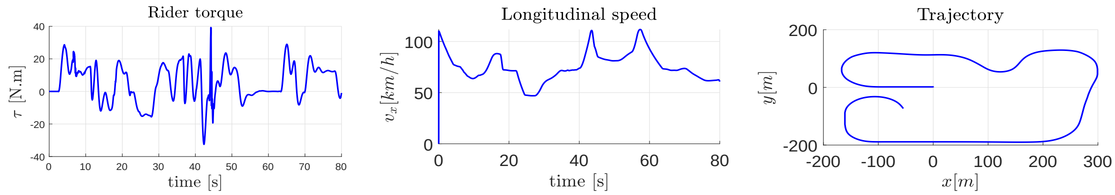

(a) (b) (c)

Fig. 2: Bikesim scenario: the rider's steering torque input τ, the forward speed v_x, and the vehicle's trajectory.

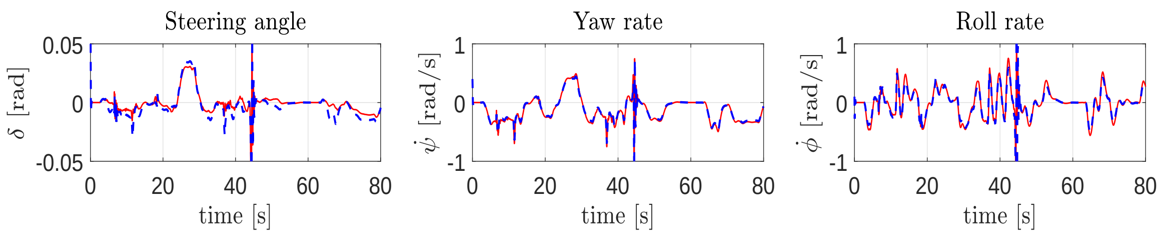

(a)

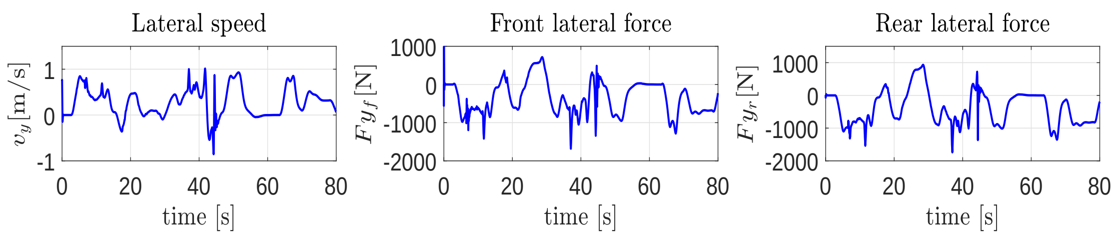

(b)

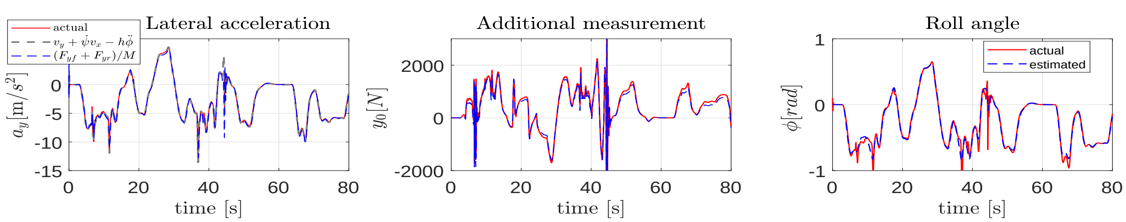

(c)

Fig. 3: Bikesim sensor (red) and observer estimation (dashed blue).

achieved since the PTWv dynamics linearization is carried out considering small roll perturbations from straight line running.

$$\hat{a}_y = \frac{(\hat{F}_{yf} + \hat{F}_{yr})}{M} \quad \text{and} \quad \hat{a}_y = \hat{\dot{v}}_y + v_x \dot{\psi} - h\hat{\ddot{\phi}}$$

Fig. 4 shows the estimated tires stiffness deviations from their nominal values. Once again, finite-time asymptotic estimation is achieved with high accuracy and the observer effectiveness is guaranteed for simultaneous states and tires' stiffness estimation. For example, for the first parameter Θ_1, the estimated deviation is used to recover the real front slip stiffness as following $C_{\alpha_f} = C_{\alpha_f,0} + \Theta_1$.

In order to make the analysis compacted, for each estimated parameters and for each method, the *Mean* value is computed among the track test. Results, summarized in Table I, show that the computed *Mean* value are generally close. It is important to remark that the parameters computed using the adaptive law are very close to nominal values, thanks to the the adaptive law used in the observer estimation. Comparing the three methods, the adaptive law has the best estimation.

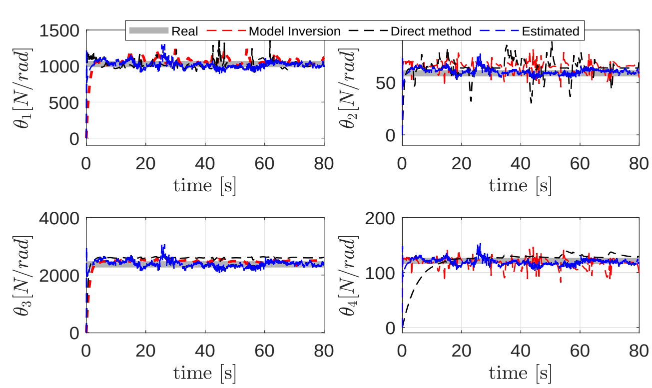

Fig. 4: Estimation performance of tire cornering stiffness.

Parameters	Nominal	Estimated	Inversion	Direct
Θ_1	1028	1022.6	1055.2	1015.7
Θ_2	58.7	60.4638	45.7477	64.2932
Θ_3	2371	2387.1	2485.3	2595.4
Θ_4	121	119.918	117.9743	124.4637

TABLE I: Parameters Mean values comparison

V. Observer Sensitivity and Robustness

This section aims to test the robustness and sensitivity of the observer with respect to the measurements' noise and regarding parameters uncertainties. Towards this end, the same test scenario, previously described is considered. Remind that the observer was designed considering the nominal tires' cornering stiffness. Consequently, there are two objectives in this section, the first is to test the observer measurement noise sensibility. The second aims to demonstrate the observer robustness to parameters variation.

A. Observer sensitivity against sensors' noise

In practice, the IMU measurements are highly affected by noises. In order to test the observer robustness in the presence of measurements noise, we consider a $5-10\%$ random perturbation on the IMU measurements. An overview of the resulting observer performances is depicted in Fig. 5.

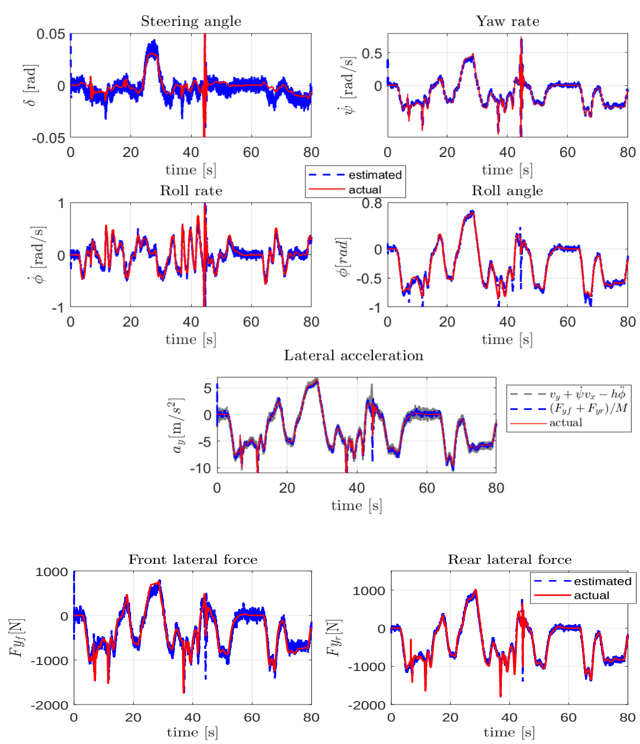

Fig. 5: Robustness to noise: observer states estimation in presence of IMU measurments noise.

It can be noted that the effect of the noise on the states estimation is limited, however, it remains slightly visible. Also, we note that the steering angle and the front tire force are most affected by noise measurements. It reveals also that the rear tire force and the roll angle are less sensitive to measurement noises.

The different noise sensitivities between the front and rear tire forces is explained by the fact that the steering dynamics mostly affects the front tire dynamics. For better performances, the estimated signals can be denoised to remove the noise effect. To that end, a simple second-order Butterworth filter can be used. Simulation result, shows that the adaptive observer is robust enough to handle the noisy case.

B. Observer robustness against modeling uncertainties

In this section, the robustness of the state observer with its associated adaptive law against modeling uncertainties is studied. This observer is designed by considering the nominal values of the tires' stiffness, hence, it is hopeful to quantify the effect of parameters variation on the observer performance. To this end, we consider a variation of $\pm 50\%$ on the real values of the front and rear tire stiffness. Next, the robustness of the observer to the parameters uncertainties is also evaluated by considering $\pm 16.5\%$ on the design value of the front and rear mass which is equivalent to an over or an underweight of 50 Kg.

The estimated states are compared with their counterparts by means of the root mean square percentage ($\mathrm{RMSE}_{\%}$). The metric quantifies the amount of error to show how close the estimated values are to the true data, $\mathrm{RMSE}_{\%}$ is defined as:

$$\mathrm{RMSE}_{\%} = \sqrt{\frac{1}{N_{\text{dataset}}} \sum_{i=1}^{N_{\text{dataset}}} (y_{\text{mes}} - y_{\text{est}})^2} \tag{39}$$

where y_{mes} is the measurement of y including N_{dataset} data points and y_{est} is its estimate provided by the observer. The resulting ($\mathrm{RMSE}_{\%}$) for the the present scenario are shown in tables II.

From table II, the $RMSE$ values for $(\dot{\phi}, \dot{\psi}, \delta, \phi, a_y)$ raise with parameters variation. Otherwise, it can be seen that the $RMSE$ for tires' stiffness parameters remain approximately constant, so, the observer is more robust for tire parameters uncertainty. Therefore, the estimated values are generally small and does not exceed 10.87% between the proposed observer and actual data. As a result, the observer gives better estimation for the nominal case, where the $RMSE$ values are the lowest. However, even with variations of the tires' parameters or the vehicle's mass, these errors are always lowers than 13% which confirms that the performances of the observer are preserved even in the presence of parametric uncertainties. Despite modeling errors between synthesis model and data from simulator, the estimation error dynamics still have good performances and the observer ensures a good estimation.

VI. Motorcycle Experimental test

In this section, an assessment of the LPV-adaptive observer performance is presented using experimental log-data. The test is carried out on an urban scenic road and performed with normal riding behavior and good environmental conditions. As depicted in Fig. 6a, the road is composed of straight lines

	RMSE				
State	*Nominal*	M^+	M^-	$C_{fr_i} \times 1.5$	$C_{fr_i} \times 0.5$
ϕ	6.195	6.369	7.9026	6.6251	7.0678
δ	1.8521	1.8965	1.7682	1.8708	1.941
$\dot{\phi}$	4.8623	6.903	7.6141	6.1901	5.589
$\dot{\psi}$	8.5218	10.467	9.1085	9.0992	9.114
a_y	9.69	11.8859	13.7928	10.8682	10.66

TABLE II: Robustness to motorcycle mass ($M^+ = M + 50$, $M^- = M - 50$), and tire parameters variation (C_{fr_i}).

followed by a narrow turns and just after a big turns. This configuration allows to solicit the PTWv roll dynamics and to maximize as possible as the persistency condition.

Fig. 8: Scooter.

Experimentation is carried-out by using a fully electric propulsion scooter of Fig. 8. The rear suitcase encloses an Intel Core i7-3610QM embedded computer manufactured by Neousys Technology dedicated to embedded applications, which also integrates a GPS receiver to measure the speed and position of the PTWv. A digital-analogue input-output card from National Instrument is plugged to interface the various sensors and actuators. On the other hand, a high-end Inertial Measurement Unit, SBG IG-500A is installed near the rear body center of mass. It incorporates an accelerometer, a gyroscope and a magnetometer providing an accurate measurements of the three Euler angles and their associated rates and the three axes acceleration. Also, the steering system is equipped with an IOV GA210 absolute encoder directly installed on the steering column without reduction stage, and offering a 10-bit resolution for 1024 steps per revolution. Data acquisition is performed at 100 Hz except for the computer-integrated GPS which is slower with a maximum frequency of 10 Hz [31].

In Fig. 7a, estimated steering angle, yaw rate and roll rate are compared to their respective measurements provided by the various sensors previously described. Once again, since these states variables are measured, we obtain a finite-time exact convergence. On the other hand, Fig. 7c reports the estimation of unmeasured state variables namely the lateral velocity v_y and the front/rear tire forces F_{yf}, F_{yr}. For validation, the estimation of unmeasured states are used to reconstruct the lateral acceleration a_y at the center of mass of the rear body G_r as shown in Fig. 7b. Fig. 9 shows the estimated tires stiffness deviations from their nominal values.

According to these results, it can be seen that the observer has a good dynamic transition and a finite-time convergence even for a riding scenario in the roll region away from the straight line dynamics linearization. In the experimental maneuver, it can be appreciated that the proposed observer shows a good estimation, however we note that the transient performance suffers slightly. It should be noted that in this maneuver, the true effective cornering stiffness should fluctuate somewhat.

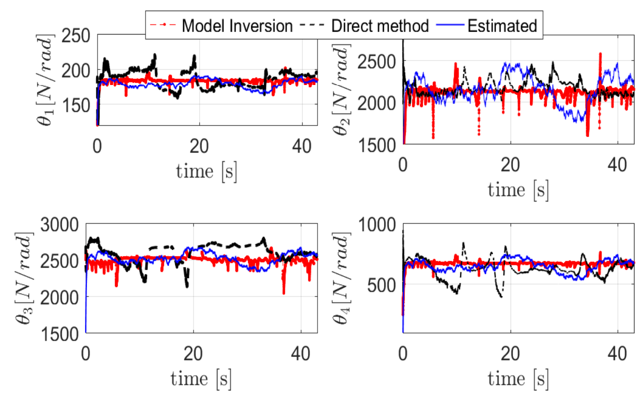

Fig. 9: Estimation performance of tire cornering stiffness.

In the experimental maneuver, it should be noted that, the true effective cornering stiffness are unknown. For more faithful estimations, the mean values of the estimated parameters are given in Table III to quantify the performances of the observer adaptive law through the mean values comparison. Comparing the adaptive law with the two others methods, one can see the small difference on the mean values results

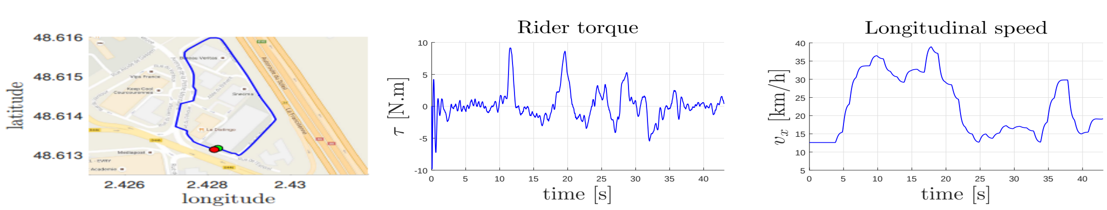

Fig. 6: Vehicle trajectory, rider steering torque and longitudinal velocity.

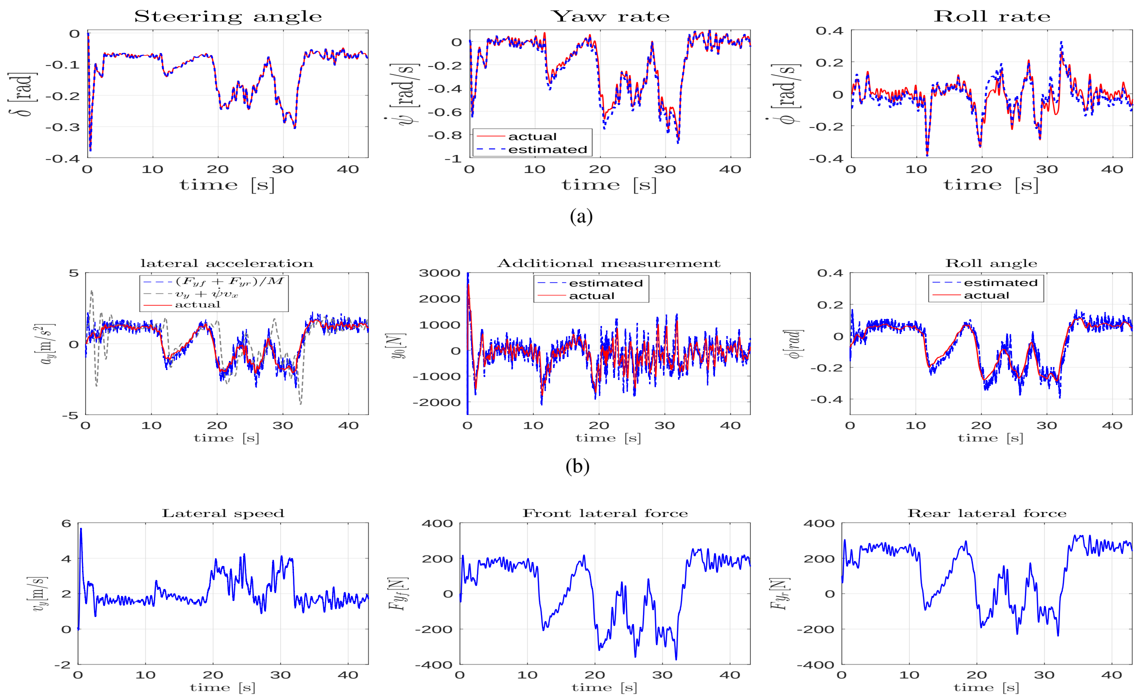

(a)

(b)

(c)

Fig. 7: Real measurements (red) and observer estimation (dashed blue).

between estimated parameters, direct and inversion methods. This confirms the performance of the estimation scheme.

Parameters	**Estimated**	**Inversion**	**Direct**
Θ_1	178.6438	181.7665	184.5632
Θ_2	2134	2065.7	2173.9
Θ_3	2513	2496	2589.3
Θ_4	643.2011	658.8327	618.1787

TABLE III: Scooter Parameters Mean values comparison

VII. Conclusion

This paper deals with observer-based identification framework to estimate both motorcycle lateral dynamic states and tires' cornering stiffness. Our main contribution concerns the design of an LPV-adaptive observer adapted to a class of systems in the context of ADAS design. For that purpose, an adaptive law is proposed, associated with an LPV formulation to deals with the variable measured longitudinal velocity. An optimization problem in forms of LMI is resolved to compute the states observer gains.

An evaluation methodology based on a co-simulation with a high-end motorcycle simulator and with real experimental data-log are presented and discussed. The fundamental evaluation is made by estimating the tires' cornering stiffness using the adaptive law, a direct method and an inversion dynamic system. The direct method is simple and straightforward but it is very sensitive to states differentiation and singularities. The inversion based algebraic method requires the computation of the outputs derivatives which can be obtained for example by a high-gain second-order sliding mode observer. This method might be unrealistic in practical applications where measurements suffer noises and disturbances, leading also to singularities in the solution of the inverse problem. The LPV-adaptive observer achieves a good estimation of unmeasured states and unknown parameters vector starting from self-integrated PTWv sensors.

Future works will be dedicated to the improvements of the observer performance by adding the rider motion and taking into account road geometry which has been considered flat.

Acknowledgments

This work has been supported by ANR project : VIROLO++ and *Informatics, Integrative Bio-Informatics and Complex Systems Laboratory* (IBISC), *Evry Val d'Essonne (UEVE)-Paris-Saclay University*.

TABLE IV: Numerical values

$M = 303.31$			
$e_{34} = 6.32$	$e_{35} = 171.38$	$e_{36} = 0.187$	$e_{44} = 34.73$
$e_{45} = 1.97$	$e_{46} = 0.66$	$e_{55} = 118.02$	$e_{56} = 0.383$
$e_{66} = 0.614$			
$\bar{a}_{34} = -303.31v_x$	$\bar{a}_{44} = -6.319v_x$	$\bar{a}_{45} = -3.665v_x$	$\bar{a}_{46} = 0.682v_x$
$\bar{a}_{47} = 0.856$	$\bar{a}_{48} = -0.624$	$\bar{a}_{51} = 1681$	$\bar{a}_{52} = 164.34$
$\bar{a}_{54} = -175.048v_x$	$\bar{a}_{56} = -1.4622v_x$	$\bar{a}_{61} = 164.34$	$\bar{a}_{62} = 69.45$
$\bar{a}_{64} = -0.8685v_x$	$\bar{a}_{65} = 1.47v_x$	$\bar{a}_{66} = -12.67$	$\bar{a}_{67} = -0.0894$
$\bar{a}_{71} = -5319v_x$	$\bar{a}_{72} = 104503v_x$	$\bar{a}_{73} = -112430$	$\bar{a}_{740} = -84997$
$\bar{a}_{760} = 10051$	$\bar{a}_{77} = -5v_x$	$\bar{a}_{81} = 3221.8v_x$	$\bar{a}_{83} = -100890$
$\bar{a}_{84} = 79098v_x$	$\bar{a}_{88} = -5v_x$		

TABLE V: Matrices expression and data

$e_{33} = M$	$e_{34} = M_f k$
$e_{35} = M_f j + M_r h$	$e_{36} = M_f e$
$e_{44} = M_f k^2 + I_{rz} + I_{fx} \sin^2 \varepsilon + I_{fz} \cos^2 \varepsilon$	
$e_{45} = M_f jk - C_{rxz} + (I_{fz} - I_{fx}) \sin \varepsilon \cos \varepsilon$	
$e_{46} = M_f ek + I_{fz} \cos \varepsilon$	
$e_{55} = M_f j^2 + M_r h^2 + I_{rx} + I_{fx} \cos^2 \varepsilon + I_{fz} \sin^2 \varepsilon$	
$e_{56} = M_f e j + I_{fz} \sin \varepsilon$	$e_{66} = I_{fz} + M_f e^2$
$\bar{a}_{34} = -M v_x$	$\bar{a}_{44} = -M_f k v_x$
$\bar{a}_{45} = \left(\frac{i_{fy}}{R_f} + \frac{i_{ry}}{R_r} \right) v_x$	$\bar{a}_{46} = \frac{i_{fy}}{R_f} \sin \varepsilon v_x$
$\bar{a}_{47} = l_f$	$\bar{a}_{48} = -l_r$
$\bar{a}_{51} = (M_f j + M_r h) g$	$\bar{a}_{52} = M_f eg - \eta Z_f$
$\bar{a}_{54} = -\left(M_f j + M_r h + \frac{i_{fy}}{R_f} + \frac{i_{ry}}{R_r} \right) v_x$	
$\bar{a}_{56} = -\frac{i_{fy}}{R_f} \cos \varepsilon v_x$	$\bar{a}_{61} = M_f eg - \eta Z_f$
$\bar{a}_{62} = (M_f eg - \eta Z_f) \sin \varepsilon$	$\bar{a}_{67} = -\eta$
$\bar{a}_{64} = -\left(M_f e + \frac{i_{fy}}{R_f} \sin \varepsilon \right) v_x$	$\bar{a}_{66} = -K$
$\bar{a}_{65} = \frac{i_{fy}}{R_f} \cos \varepsilon v_x$	$\bar{a}_{71} = \frac{C_{f2}}{\sigma_f} v_x$
$\bar{a}_{72} = \frac{1}{\sigma_f} \left(C_{f1} \cos \varepsilon + C_{f2} \sin \varepsilon \right) v_x$	
$\bar{a}_{73} = -\frac{C_{f1}}{\sigma_f}$	$\bar{a}_{74} = -\frac{C_{f1}}{\sigma_f} l_f$
$\bar{a}_{76} = \frac{C_{f1}}{\sigma_f} \eta$	$\bar{a}_{77} = -\frac{1}{\sigma_f} v_x$
$\bar{a}_{81} = \frac{C_{r2}}{\sigma_r} v_x$	$\bar{a}_{83} = -\frac{C_{r1}}{\sigma_r}$
$\bar{a}_{84} = \frac{C_{r1}}{\sigma_r} l_r$	$\bar{a}_{88} = -\frac{1}{\sigma_r} v_x$
$c_{57} = \frac{1}{M}$	$c_{57} = \frac{1}{M}$
$c_{67} = M_f k - M l_f$	$c_{68} = M_f k + M l_r$

TABLE VI: Motorcycle dynamics variables

symbol	signification
v_x, v_y	longitudinal and lateral speeds
ϕ, ψ, δ	roll, yaw, steering angles
$\dot{\phi}$, $\dot{\psi}$, $\dot{\delta}$	roll, yaw, steering rates
F_{yf}, F_{yr}	cornering front and rear forces
τ, a_y	rider torque and lateral acceleration
M_f , M_r , M	front and rear body mass
j, h, k, e, l_f, l_r	linear dimensions
i_{fy}, i_{ry}	polar moment of inertia of wheels
R_f, R_r	front and rear wheel radius
ε, η, K	caster angle, trail, damper coefficient
I_f, I_r	front and rear body inertia
g, Z_f	gravity acceleration and front vertical force
σ_f, σ_r	front and rear tire relaxation

$$\bar{E} = \begin{bmatrix} 1 & 0 & 0 & 0 & 0 & 0 & 0 & 0 \\ 0 & 1 & 0 & 0 & 0 & 0 & 0 & 0 \\ 0 & 0 & e_{33} & e_{34} & e_{35} & e_{36} & 0 & 0 \\ 0 & 0 & e_{34} & e_{44} & e_{45} & e_{46} & 0 & 0 \\ 0 & 0 & e_{35} & e_{45} & e_{55} & e_{56} & 0 & 0 \\ 0 & 0 & e_{36} & e_{46} & e_{56} & e_{66} & 0 & 0 \\ 0 & 0 & 0 & 0 & 0 & 0 & 1 & 0 \\ 0 & 0 & 0 & 0 & 0 & 0 & 0 & 1 \end{bmatrix} \bar{B} = \begin{bmatrix} 0 \\ 0 \\ 0 \\ 0 \\ 0 \\ 1 \\ 0 \\ 0 \end{bmatrix}$$

$$\bar{A}(v_x) = \begin{bmatrix} 0 & 0 & 0 & 0 & 1 & 0 & 0 & 0 \\ 0 & 0 & 0 & 0 & 0 & 1 & 0 & 0 \\ 0 & 0 & 0 & a_{34} & 0 & 0 & 1 & 1 \\ 0 & 0 & 0 & a_{44} & a_{45} & a_{46} & a_{47} & a_{48} \\ a_{51} & a_{52} & 0 & a_{54} & 0 & a_{56} & 0 & 0 \\ a_{61} & a_{62} & 0 & a_{64} & a_{65} & a_{66} & a_{67} & 0 \\ a_{71} & a_{72} & a_{73} & a_{74} & 0 & a_{76} & a_{770} & 0 \\ a_{81} & 0 & a_{83} & a_{84} & 0 & 0 & 0 & a_{88} \end{bmatrix}$$

$$C = \begin{bmatrix} 0 & 1 & 0 & 0 & 0 & 0 & 0 & 0 \\ 0 & 0 & 0 & 1 & 0 & 0 & 0 & 0 \\ 0 & 0 & 0 & 0 & 1 & 0 & 0 & 0 \\ 0 & 0 & 0 & 0 & 0 & 1 & 0 & 0 \\ 0 & 0 & 0 & 0 & 0 & 0 & c_{57} & c_{58} \\ 0 & 0 & 0 & 0 & 0 & 0 & c_{67} & c_{68} \end{bmatrix}$$

References

[1] M. Corno, G. Panzani, and S. M. Savaresi, “Traction-control-oriented state estimation for motorcycles,” *IEEE Transactions on Control Systems Technology*, vol. 21, no. 6, pp. 2400–2407, 2013.

[2] A. Teerhuis and S. Jansen, “Motorcycle state estimation for lateral dynamics,” *Vehicle system dynamics*, vol. 50, no. 8, pp. 1261–1276, 2012.

[3] P. De Filippi, M. Corno, M. Tanelli, and S. M. Savaresi, “Single-sensor control strategies for semi-active steering damper control in two-wheeled vehicles,” *IEEE Transactions on Vehicular Technology*, vol. 61, no. 2, pp. 813–820, 2012.

[4] I. Boniolo, S. M. Savaresi, and M. Tanelli, “Lean angle estimation in two-wheeled vehicles with a reduced sensor configuration,” in *Circuits and Systems (ISCAS), 2012 IEEE International Symposium on*, pp. 2573–2576. IEEE, 2012.

[5] M. Corno, S. M. Savaresi, and G. J. Balas, “On linear-parameter-varying (lpv) slip-controller design for two-wheeled vehicles,” *International Journal of Robust and Nonlinear Control: IFAC-Affiliated Journal*, vol. 19, no. 12, pp. 1313–1336, 2009.

[6] M. E.-H. Dabladji, D. Ichalal, H. Arioui, and S. Mammar, “On the estimation of longitudinal dynamics of powered two-wheeled vehicles,” in *Control Conference (ECC), 2015 European*, pp. 921–926. IEEE, 2015.

[7] C. Chabane, D. Ichalal, H. Arioui, and S. Mammar, “Proportional two integral (p2i) observer synthesis for single track vehicle,” in *20th Mediterranean Conference on Control and Automation (MED 2012)*, pp. 1530–1535, 2012.

[8] H. Guo, D. Cao, H. Chen, C. Lv, H. Wang, and S. Yang, “Vehicle dynamic state estimation: state of the art schemes and perspectives,” *IEEE/CAA Journal of Automatica Sinica*, vol. 5, no. 2, pp. 418–431, 2018.

[9] M. Zhou, Z. Cao, M. Zhou, J. Wang, and Z. Wang, “Zonotoptic fault estimation for discrete-time lpv systems with bounded parametric uncertainty,” *IEEE Transactions on Intelligent Transportation Systems*, 2019.

[10] S. M. Savaresi, M. Tanelli, P. Langthaler, L. Del Re *et al.*, “New regressors for the direct identification of tire deformation in road vehicles via” in-tire” accelerometers,” *IEEE Transactions on Control Systems Technology*, vol. 16, no. 4, pp. 769–780, 2008.

[11] S. Savaresi, M. Tanelli, P. Langthaler, and L. Del Re, “Identification of tire-road contact forces by ”in-tire” accelerometers,” in *14th IFAC Symposium on System Identification*, pp. 1–6, 2006.

[12] R. Hildebrand and M. Gevers, “Identification for control: optimal input design with respect to a worst-case ν-gap cost function,” *SIAM Journal on Control and Optimization*, vol. 41, no. 5, pp. 1586–1608, 2002.

[13] A. Dixit and S. Suryanarayanan, “Adaptive observers for servo systems with friction,” in *Control Applications, 2008. CCA 2008. IEEE International Conference on*, pp. 960–965. IEEE, 2008.

[14] P. Garimella and B. Yao, “Nonlinear adaptive robust observer design for a class of nonlinear systems,” in *American Control Conference, 2003. Proceedings of the 2003*, vol. 5, pp. 4391–4396. IEEE, 2003.

[15] Y. Wang, L. Zhou, S. A. Bortoff, A. Satake, and S. Furutani, “An approximate high gain observer for speed-sensorless estimation of induction motors,” *IEEE/CAA Journal of Automatica Sinica*, vol. 6, no. 1, pp. 53–63, 2018.

[16] S. Zhu, X. Wang, and H. Liu, “Observer-based iterative and repetitive learning control for a class of nonlinear systems,” *IEEE/CAA Journal of Automatica Sinica*, vol. 5, no. 5, pp. 990–998, 2017.

[17] R. S. Sharp, “The stability and control of motorcycles,” *Journal of mechanical engineering science*, vol. 13, no. 5, pp. 316–329, 1971.

[18] C. Sierra, E. Tseng, A. Jain, and H. Peng, “Cornering stiffness estimation based on vehicle lateral dynamics,” *Vehicle System Dynamics*, vol. 44, no. sup1, pp. 24–38, 2006.

[19] M. Zhang, Z.-t. Li, M. Cabassud, and B. Dahhou, “Unknown input reconstruction: A comparison of system inversion and sliding mode observer based techniques,” in *Control Conference (CCC), 2017 36th Chinese*, pp. 7172–7177. IEEE, 2017.

[20] M. Weiss, F. Baret, R. Myneni, A. Pragnère, and Y. Knyazikhin, “Investigation of a model inversion technique to estimate canopy biophysical variables from spectral and directional reflectance data,” *Agronomie*, vol. 20, no. 1, pp. 3–22, 2000.

[21] S. Roychowdhury, M. Zhao, A. Wallin, N. Ohlsson, and M. Jonasson, “Machine learning models for road surface and friction estimation using front-camera images,” in *2018 International Joint Conference on Neural Networks (IJCNN)*, pp. 1–8. IEEE, 2018.

[22] H. Liu, X. Song, T. Nanayakkara, K. Althoefer, and L. Seneviratne, "Friction estimation based object surface classification for intelligent manipulation," in *IEEE International Conference on Robotics and Automation*, 2011.
[23] J. C. Sanchez, F. Gavilan, R. Vazquez, and C. Louembet, "A Flatness-Based Predictive Controller for Six-Degrees of Freedom Spacecraft Rendezvous," in *IFAC Workshop on Networked & Autonomous Air & Space Systems*, Santa Fe, Nouveau Mexique, United States, Jun. 2018.
[24] A. Levant, "Higher-order sliding modes, differentiation and output-feedback control," *International journal of Control*, vol. 76, no. 9-10, pp. 924–941, 2003.
[25] A. Belov, S. Aranovskiy, R. Ortega, N. Barabanov, and A. Bobtsov, "Enhanced parameter convergence for linear systems identification: The drem approach," in *2018 European Control Conference (ECC)*, pp. 2794–2799. IEEE, 2018.
[26] A. Pertew, H. Marquez, and Q. Zhao, "Design of unknown input observers for lipschitz nonlinear systems," in *American Control Conference, 2005. Proceedings of the 2005*, pp. 4198–4203. IEEE, 2005.
[27] L. Xie, "Output feedback H_∞ control of systems with parameter uncertainty," *International Journal of control*, vol. 63, no. 4, pp. 741–750, 1996.
[28] M. Corless and J. Tu, "State and input estimation for a class of uncertain systems," *Automatica*, vol. 34, no. 6, pp. 757–764, 1998.
[29] K. Tanaka and H. O. Wang, *Fuzzy control systems design and analysis: a linear matrix inequality approach*. John Wiley & Sons, 2004.
[30] R. Sharp, S. Evangelou, and D. J. Limebeer, "Advances in the modelling of motorcycle dynamics," *Multibody system dynamics*, vol. 12, no. 3, pp. 251–283, 2004.
[31] P.-M. Damon, D. Ichalal, L. Nehaoua, and H. Arioui, "Lateral & steering dynamics estimation for single track vehicle: Experimental tests," *IFAC-PapersOnLine*, vol. 50, no. 1, pp. 3400–3405, 2017.

Majda FOUKA received the Dipl.-Ing. degree and the Master's degree in automatic and control systems from the The National Polytechnic School of Alger, Algeria, in 2015; the M.S. degree in Automatic and application from National Higher Engineering School of Poitiers (ENSIP), France and the Ph.D. degree in automatic from the University of Evry Val d'Essonne-Paris Saclay, Evry, France, in 2019. She is currently Associate Professor in automatic and electrical engineering with the Informatics, Integrative Biology and Complex Systems Laboratory, Université d'Evry Val-d'Essonne, Evry, France. Her main research interests include rider assistance, state and parameters estimation and observer design of nonlinear systems with special focus on the fields of two-wheeled vehicles.

Lamri NEHAOUA received the B.S. degree in engineering on control and automation systems science from the University of Sétif, Sétif, Algeria, in 1999, the M.S. degree in computer vision for robotics applications from Clermont-Ferrand II University, Clermont-Ferrand, France, in 2002, and the Ph.D. degree from the University of Evry Val d'Essonne, Evry, France, in 2008 then a a postdoctoral position with the Informatics, Integrative Biology and Complex Systems Laboratory, University of Evry. He currently holds an Associate Professor with Université d'Evry Val-d'Essonne. His research interests are driving simulators, driver assistance, modeling, control, and observation of complex systems

Hichem ARIOUI received the Dipl.-Ing. degree on control systems from Badji Mokhtar University, Annaba, Algeria, in 1998 and the M.S. and Ph.D. degrees in robotics and automation from Université d'Evry Val-d'Essonne, Evry, France, in 1999 and 2002, respectively. Then, he was with the Informatics, Integrative Biology and Complex Systems Laboratory, Université d'Evry Val-d'Essonne, where he worked on the control of haptic display under varying time delay in the frame of his Ph.D. dissertation. Since 2003, he has been an Associate Professor of electrical engineering with Université d'Evry Val-d'Essonne. His research interests include modeling and control of haptic interaction and, more recently, the design and control of driving simulator applications.